POLITECNICO
MILANO 1863

SCUOLA DI INGEGNERIA INDUSTRIALE
E DELL'INFORMAZIONE

Executive Summary of the Thesis

Large Eddy Simulations of a Lean Premixed Swirl-stabilized Combustor

Laurea Magistrale in Energy Engineering - Ingegneria Energetica

Author: Giacomo Abbasciano

Advisor: Prof. Dr. Giacomo Bruno Azzurro Persico

Co-advisor: Prof. Dr. Ivan Langella

Academic year: 2022-2023

1. Introduction

Hydrogen, with its high energy density and carbon-free combustion, is a promising clean energy carrier for power generation and potential use in aeronautics. Stabilizing hydrogen flames in ultra-lean premixed conditions, exploiting its wide flammabiity range, can suppress nitric oxides (NO_x) formation linked to high flame temperatures via the Zel'dovich mechanism. Swirled combustors are commonly used to rapidly mix and stabilize lean premixed flames, particularly in low-velocity regions associated to the central recirculation zone. The high reactivity and diffusivity of hydrogen pose challenges such as flashback and flame instabilities. To address this, axial air injection (AAI) can be employed to increase axial momentum within the combustor, effectively controlling flame positioning and preventing flashback [4, 5]. In the present work, large eddy simulations (LES) with flamelets based thermochemistry and presumed probability density function (PDF) to represent the flame-turbulence interaction, are used to investigate the flow field and emissions within the swirled technically premixed laboratory combustor with AAI at TU Delft. The objective of the present work is to assess the ability of the in-house developed LES model to predict the correct flow field and pollutant emissions in the swirled flow configuration, in order to facilitate future investigation of hydrogen-enriched flames. The study is organised as follows. First, a non-reactive case with only oxidizer as working fluid is analyzed to validate the model against in house experimental data, and to achieve further insight on the flow features and its dependence on the swirl number at the inlet of the mixing tube. The analysis is then extended to a non-reactive CH_4/air to understand how density variation affects flow features. Finally, a reactive CH_4/air is simulated to evaluate the LES closure and an innovative NO_x emission prediction method.

2. Unclosed terms and their modeling

2.1. Turbulence modeling

The objective of this section is to illustrate how the following terms of the reactive multicomponent Favre-Filtered N-S equations are modeled: Reynolds stresses ($\widetilde{u_i u_j} - \tilde{u}_i \tilde{u}_j$) and scalar fluxes ($\widetilde{u_j Y_k} - \tilde{u_j} \tilde{Y_k}$ and $\widetilde{u_j h_s} - \tilde{u}_j \tilde{h}_s$).

2.1.1 One-equation model

The One-equation eddy viscosity subgrid-scale (SGS) model uses the eddy viscosity approximation, which consists in modeling the subgrid-scale (viscous) stress tensor as follows [3]:

$$\overline{\rho}(\widetilde{\boldsymbol{uu}} - \tilde{\boldsymbol{u}}\tilde{\boldsymbol{u}}) = -2\nu_T \left(\widetilde{S}_{ij} - \frac{1}{3}\widetilde{S}_{kk}\delta_{ij} \right) \quad (1)$$

where ν_T is the subgrid-scale eddy viscosity (or residual viscosity), $\widetilde{S}_{ij} = \frac{1}{2}\left(\frac{\partial \widetilde{u}_i}{\partial x_j} + \frac{\partial \widetilde{u}_j}{\partial x_i}\right)$ is the Favre-filtered strain tensor (resolved strain tensor) and δ_{ij} is the Kronecker delta.
The residual viscosity is modeled in this work as:

$$\nu_T = C_v k_r^{1/2} \Delta \quad (2)$$

where Δ is the LES-filter width, C_v is a model constant whose default value is $\simeq 0.1$ and k_r is the residual kinetic energy, defined as:

$$k_r \doteq \frac{1}{2}\left(\widetilde{u_i u_i} - \widetilde{u}_i \widetilde{u}_i\right) \quad (3)$$

for which a transport equation, further analyzed in [3], is solved:

$$\bar{\rho}\frac{Dk_r}{Dt} = \frac{\partial}{\partial x_j}\left(\widetilde{\mu}\frac{\partial k_r}{\partial x_j}\right) + \widetilde{u}_i \frac{\partial \tau_{ij}^R}{\partial x_j} - \frac{\partial f_j}{\partial x_j} - \varepsilon_k + \Pi \quad (4)$$

2.1.2 Modeling of the unresolved scalar transport

As in RANS, LES unresolved scalar fluxes are often described using a gradient assumption [3], and this work is no exception:

$$\widetilde{u_j Y_k} - \tilde{u_j}\tilde{Y_k} = -\frac{\nu_t}{Sc_k}\frac{\partial \tilde{Y_k}}{\partial x_i} \quad (5)$$

where Sc_k is a subgrid-scale Schmidt number. The subgrid-scale viscosity ν_t is estimated from the unresolved Reynolds stresses models (i.e. One-equation model in this work). Since the majority of transport is addressed at large scales and only a portion needs to be represented, the gradient hypothesis in LES is effective in the majority of cases.

2.2. Combustion modeling: the Flamelet model with PDF

The particular Flamelet model used in this work is now going to be introduced. Two control variables are included for the chemistry representation: the progress variable c and the mixture fraction Z. They are sufficient since it is assumed adiabatic combustion (hence the extensive enthalpy, and not the specific enthalpy, is conserved in the combustion chamber), whereas in presence of heat losses also the enthalpy needs to be used to take this aspect into account. The interaction between chemistry and turbulence is considered through a presumed beta-shaped probability density function (PDF) approach, which is considered for the progress variable and mixture fraction and results in two extra control variables: progress variable variance and mixture fraction variance. The resulting turbulent manifold is four-dimensional, in which the dimensions are progress variable, mixture fraction, progress variable variance and mixture fraction variance. The Flamelet model has also the objective of chemistry reduction, which means not solving all the filtered species transport equations, which reduces the computational effort and solves the stiffness problem related to the reaction rate. The detailed kinetic mechanism GRI-Mech 3.0 coupled with the solver CHEM1D are used, in this sense, to build the laminar manifold.
Assuming that the progress variable and the mixture fraction are statistically independent in the flame, that allows to say $\tilde{P}(Z,c) \simeq P_\beta(Z;\tilde{Z},\widetilde{Z''^2}) \times P_\beta(c;\tilde{c},\widetilde{c''^2})$ as further explained in [**? ?**], the filtered source term of the progress variable is calculated as [**?**]:

$$\overline{\dot{\omega}_c} = \int\int \dot{\omega}_c(c,Z) P(c;\tilde{c},\widetilde{c''^2}) P(Z;\tilde{Z},\widetilde{Z''^2}) dc dZ \quad (6)$$

The reason why this Flamelet combustion model is used in this work is that it retains most of the physical accuracy of a detailed simulation while drastically reducing its computational time, paving the way for new developments of alternative fuel usage (e.g. hydrogen) in a cleaner and more efficient combustion.

3. Simplifying assumptions and working equation set

3.1. Simplifying assumptions

With regard to non-reacting problems, combustion adds complexity because species react and their rate of reaction $\dot{\omega}_k$ must be modeled, species and heat coefficients change within the solution, and transport coefficients are species-dependent. This complexity necessitates a number of simplifying assumptions. In this section the simplifying assumptions that are going to be used in this work, and their effect on the governing equations, are highlighted [1, 3, 6]:

- For subsonic flow the viscous dissipation term can be neglected, being much smaller than the heat release
- Radiative heat transfer is generally neglected, although it is relevant for certain applications with sooty flames.
- Body forces are neglected for every species.
- Dofour effect and Soret effect are generally not taken into account, the former is in fact typically negligible in most combustion problems whereas the latter is typically neglected for simplicity.
- In low-speed subsonic flow (deflagrations) the low Mach approximation can be made ($Ma << 1$): this implies that $\nabla p \simeq 0$ hence both the momentum and energy equation result to be simplified. In comparison to their compressible counterparts, LES, DNS, and RANS simulations can use greater time steps thanks to this approximation. As a result, more complex kinetics can be used, which can improve predictions of the flame and its interactions with turbulence. On the other hand, in exchange, the acoustics are ignored. The interest in this work is for deflagration flames, where the pressure is nearly constant throughout the flame and the speed of the flame front (i.e., the speed with which it advances into the reactants field) is substantially slower than the speed of sound. In the energy equation, but not the momentum equation, the effects of pressure variations can therefore be disregarded. Despite the low Mach number, the density is not constant because of the strong heat release across the flame: low Mach approximation eliminates the dependency of density on pressure $\rho(T, p, \boldsymbol{X}) = \rho(T, \boldsymbol{X})$. This means that a non-reactive mono-component case will result to be incompressible.
- The diffusion velocities can be modeled using the Hirschfelder approximation, thus one can write $\boldsymbol{V}_k X_k = -D_k \nabla X_k$, where D_k is related to the thermal diffusivity D_{th} through the Lewis number of species k: $Le_k D_k = D_{th}$ where D_{th} is the thermal diffusivity defined as $D_{th} = \dfrac{\lambda_m}{\rho c_p}$, c_p is the averaged specific heat at a constant pressure of the mixture ($c_p = \sum_{k=1}^{N} c_{p,k} Y_k$).
- The assumption of $Le_k = 1$ for all the $k-th$ species is generally made to simplify turbulent flame modeling, especially in premixed flames when species mass fractions and temperature are assumed to be equivalent variables. Nevertheless, thermo-diffusive instabilities occur in premixed systems when the Lewis number is lower than unity (e.g. for hydrogen).
- The fluid mixture is considered to be Newtonian, with zero bulk viscosity, that allows to express $\underline{\underline{\boldsymbol{\tau}}}$ as:
  $\underline{\underline{\boldsymbol{\tau}}} = 2\mu_m \left(\underline{\underline{\boldsymbol{S}}} - \frac{1}{3} div(\boldsymbol{u}) \underline{\underline{\boldsymbol{I}}} \right)$.
- It is assumed the validity of the equation of state of the ideal gas, since the temperatures with which the combustion deals are much higher than double the critical temperature of the mixture of reactants and products.
- absence of external heat sources.

3.2. Working equation set

To conclude, the tabulated FM database is connected to the OpenFOAM CFD solver. In addition to the momentum and mass balance equations, only the following transport equations are solved:

Mass

$$\frac{\partial \overline{\rho}}{\partial t} + div(\overline{\rho}\tilde{\boldsymbol{u}}) = 0 \tag{7}$$

Momentum

$$\begin{aligned} \frac{\partial \overline{\rho}\tilde{\boldsymbol{u}}}{\partial t} + div(\overline{\rho}\tilde{\boldsymbol{u}}\tilde{\boldsymbol{u}}) + \nabla \overline{p} \\ - div\left(\underline{\underline{\overline{\boldsymbol{\tau}}}} - \overline{\rho}(\widetilde{\boldsymbol{u}\boldsymbol{u}} - \tilde{\boldsymbol{u}}\tilde{\boldsymbol{u}}) \right) = 0 \end{aligned} \tag{8}$$

Filtered mixture fraction $\tilde{Z}$

$$\frac{\partial \bar{\rho}\tilde{Z}}{\partial t} + div\left(\bar{\rho}\tilde{\boldsymbol{u}}\tilde{Z}\right) = div\left(\bar{\rho}D_{\text{eff}}\nabla\widetilde{Z}\right) \quad (9)$$

(Subgrid) Variance of the mixture fraction $\widetilde{Z''^2}$

$$\frac{\partial \bar{\rho}\widetilde{Z''^2}}{\partial t} + div\left(\bar{\rho}\tilde{\boldsymbol{u}}\widetilde{Z''^2}\right) = div\left(\bar{\rho}D_{\text{eff}}\nabla\widetilde{Z''^2}\right) - 2\bar{\rho}\tilde{\chi}_{Z,\text{sgs}} + 2\bar{\rho}\frac{\nu_t}{\text{Sc}_t}|\nabla\widetilde{Z}|^2 \quad (10)$$

Filtered progress variable $\tilde{c}$

$$\frac{\partial \bar{\rho}\tilde{c}}{\partial t} + div\left(\bar{\rho}\tilde{\boldsymbol{u}}\tilde{c}\right) = div\left(\bar{\rho}D_{\text{eff}}\nabla\tilde{c}\right) + \overline{\dot{\omega}_c^*} \quad (11)$$

(Subgrid) Variance of the progress variable $\widetilde{c''^2}$

$$\frac{\partial \bar{\rho}\widetilde{c''^2}}{\partial t} + div\left(\bar{\rho}\tilde{\boldsymbol{u}}\widetilde{c''^2}\right) = div\left(\bar{\rho}D_{\text{eff}}\nabla\widetilde{c''^2}\right) - 2\bar{\rho}\tilde{\chi}_{c,\text{sgs}} + 2\bar{\rho}\frac{\nu_t}{\text{Sc}_t}|\nabla\widetilde{c}|^2 + 2\left(\overline{c\dot{\omega}_c^*} - \widetilde{c}\overline{\dot{\omega}_c^*}\right) \quad (12)$$

where ν and ν_t are the filtered molecular and subgrid-scale viscosities respectively (the former retrieved from the 4-D manifold and the latter computed with the One-Equation model). D_{eff} is the effective mixture diffusivity modelled as $D_{eff} = \tilde{D} + \nu_t/Sc_t$, where Sc_t is a turbulent Schmidt number and $\tilde{D} = \tilde{\nu}/Sc$ is the filtered molecular diffusivity. The subgrid-scale scalar dissipation rate (SDR) of the mixture fraction is modeled as $\bar{\rho}\tilde{\chi}_{Z,\text{ sgs}} = C_Z\bar{\rho}\left(\nu_t/\Delta^2\right)\widetilde{Z''^2}$ where C_Z is a constant and Δ is the LES-filter width. In the present work, also the total enthalpy (i.e. sensible + formation) is transported through solving the balance equation (13), and not retrieved from the look-up table:

$$\frac{\partial \bar{\rho}\tilde{h}}{\partial t} + div(\bar{\rho}\tilde{\boldsymbol{u}}\tilde{h}) = div\left[\bar{\rho}\left(\frac{\tilde{\nu}}{\text{Pr}} + \frac{\nu_t}{\text{Pr}_t}\right)\nabla\tilde{h}\right] + \frac{\overline{Dp}}{Dt} \quad (13)$$

Note that in order to include the compressibility effects in the simulation, the Favre-filtered transport equation for the total enthalpy including the pressure effect is considered. Pr and Pr_t are the laminar and turbulent Prandtl numbers (both set to 0.7) and $\frac{\overline{Dp}}{dt}$ is the filtered substantial derivative of pressure, given by: $\frac{\overline{Dp}}{dt} \simeq \frac{\partial \overline{p}}{\partial t} + \tilde{\boldsymbol{u}} \cdot \nabla\overline{p}$.

4. Results

4.1. Non reactive unfueled case

4.1.1 Methodology

It is important to notice the manner in which the boundary condition for the velocity field has been established. The flow field can be extracted at the same location from a Large Eddy Simulation that encompasses the swirler, serving as the inlet for the LES domain. This approach is used to effectively capture the physics of the swirling flow. This approach is also used to avoid the need of simulating the swirler, which requires cells of such small size that the time step must be limited in order to maintain the Courant-Friedrichs-Lewy (CFL) condition below the predetermined threshold. Consequently, this leads to an unacceptably long simulation time. To achieve this objective, an inflow turbulence generator is used in order to generate a flow field that has the same mean and variance as the extracted field. The flow field obtained is post processed using Matlab, enabling the scaling of both the bulk velocity, and as a consequence the axial component of velocity, and the azimuthal component of the velocity. The adjustment of the tangential velocity is achieved by the implementation of a scaling factor, which then alters the swirl number of the fluid as it exits the swirler and enters the mixing tube. The bulk velocity is adjusted to enforce the nominal mass flow rate, resulting in a fixed value. Consequently, the only determining factor for altering the swirl number is the azimuthal velocity. The altered flow field is now enforced at the inlet of the domain as a boundary condition.

The generation of the inlet flow field is a crucial step in cases where the swirler is not being solved. This is due to the turbulent nature of the flow, characterized by a Reynolds number of around 6000 in the analyzed combustor under the set conditions. It is important to note

that this value is much higher than the laminar-turbulent transition threshold of 2300 for the internal pipe's shape. Additionally, the flow exhibits swirling motion. Due to this rationale, both the boundary conditions of mass flow rate and bulk velocity are deemed unsuitable since they would enforce a non-swirling laminar flow. In conclusion, the ability to manipulate the swirl number by adjusting the azimuthal component allows for a sensitivity analysis on the Swirl number.
A total of five cases have been simulated, as illustrated in Table 1.

LES	$V_\theta \nearrow$	$U_{axial} \nearrow$
LES 0% (Base Case)	0%	0%
LES 10%	10%	0%
LES 15%	15%	0%
LES 50%	50%	0%
LES 80%	80%	0%

Table 1: Overview of non-reactive full air LESs.

The swirl number distribution along the mixing tube for all cases is shown in figure 1.

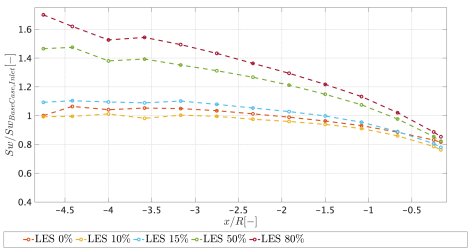

Figure 1: Swirl number along the mixing tube varying V_{tang}.

4.1.2 Sensitivity analysis on the Swirl number

Figure 2 shows that when the tangential velocity adjustment is increased by 50%, a high level of accuracy is attained for all streamwise locations. The cross-sectional slice denoted as $x/R = 1$ demonstrates a precise prediction of the central recirculation zone, while also exhibiting a consistent aperture of the jet with the experimental observations. The peaks of axial velocity exhibit greater magnitudes in comparison to the other LESs, mostly due to the intensified reverse flow and the need for the mass to conserve. The LES model with a 50% adjustment has the highest level of agreement with the experimental PIV data, demonstrating a notable accuracy in its ability to forecast the flow field. Therefore, the adjustment of the azimuthal component of the velocity will be maintained for the further examination of TUDelft's combustor in this study.

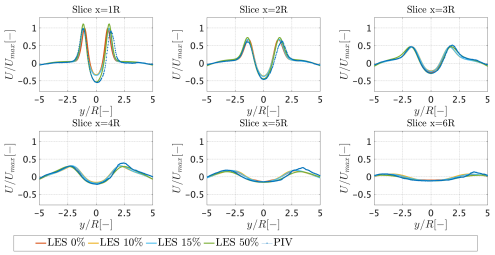

Figure 2: Figure 6.9: LES Favre-filtered time-averaged radial distribution of the axial velocity against PIV.

4.2. Validation

The axial velocity distribution in the first six radiuses of the combustion chamber for $LES50\%$ and PIV is shown in Figure 3. The agreement about the jet's aperture, strength of the CRZ, and the effectiveness of capturing the vorticity, especially in the outer recirculation zone, is remarkable.

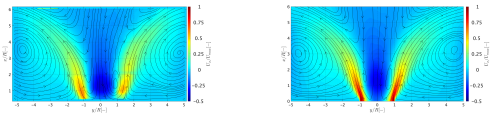

(a) PIV. (b) LES

Figure 3: Colormap representing a) PIV axial velocity b) the axial velocity of the LES 50% in the combustion chamber. Streamlines are depicted for the velocity field.

4.3. Non reactive methane case

A non-reactive full methane LES is employed to investigate the impact of density fluctuation on the flow field generated by swirling flow, with the aim of enhancing our knowledge in this regard. The density of air is specifically modified by a 4% increment using the inflow turbulence gen-

erator, and the examination of the flow field involves a comparison between LES and PIV data. The density of methane is kept unaltered due to its lack of influence, mostly attributed to the air-to-fuel ratio exceeding 20 on a mass basis at the set equivalency ratio. Moreover, the characteristics of the fuel are determined by the comprehensive chemical data provided in tabular form, making it impractical to intervene in that regard.

4.3.1 Validation against PIV

Figure 4 presents a comparison of the radial profile of axial velocity between LES and PIV. On one hand, it is anticipated that the axial velocity would be comparatively lower than that of experiments as a result of the increased air density that is applied. In contrast, it can be shown from figure 4 that the LES method yields greater values for axial velocities, especially in $x/R = 1$.

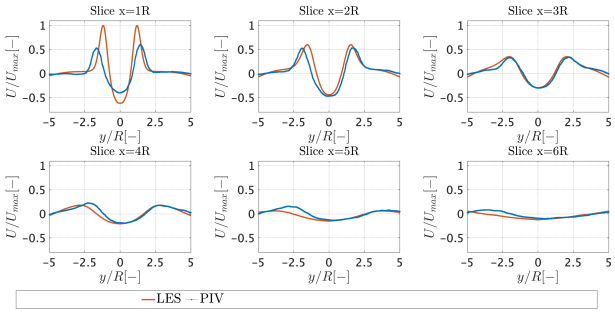

Figure 4: LES Favre-filtered time-averaged radial distribution of the axial velocity against PIV.

Three causes have been identified to explain the discrepancy:

- The temperature field exhibits a value that surpasses the prescribed boundary condition, despite the absence of any reactions (i.e., absence of heat release) and the adiabatic assumption of the case. Upon examination of the scatterplots depicting the enthalpy of formation obtained from the thermochemistry tabulation, it becomes evident that the observed trend within the flammability limits of methane is non-linear. This non-linearity indicates that the representation of the methane-air mixture is inadequate, leading to temperature oscillations. The elevated $\langle \tilde{T} \rangle$ inside the mixing tube, which attains a maximum value of 10% relative to the boundary condition, results in the expansion of the mixture, hence causing acceleration. However, the acceleration resulting from this expansion is insufficient to account for the observation that the velocity peak of the LES is twice as high as that of the PIV at $x/R = 1$. A 10% deviation in temperature would result in a 10% reduction in density according to the ideal gas equation of state. Consequently, the acceleration of the flow would increase by 10% in accordance with the principle of mass conservation. Hence, this discrepancy of 100% cannot be accounted for only by the aforementioned explanation.
- On one side, the introduction of a density augmentation would likely result in a reduction of the velocity peaks. Consequently, a reduction in the axial flow of axial momentum would occur, resulting in an augmentation of the swirl number at the inlet of the combustion chamber, so initiating a more intense vortex breakdown phenomenon. Consequently, an elevated axial component of the negative pressure gradient along the centerline would give rise to a stronger reverse flow, so mitigating the impact of increased density on the reduction in axial velocity, and possibly leading to a lower negative value (i.e. higher in magnitude) for the axial velocity in the CRZ.
- It is possible that the radial component of the gradient of mixture fraction in the vicinity of $x = 1R$ exhibits an elevated value compared to the experimental observed behavior. The experimental findings indicate that the fuel-air mixture inside the center of the jet is leaner, while it becomes richer in the outer shear layer. This implies that the LES model would predict a less effective mixing compared to the actual observed mixing. Undoubtedly, a leaner mixture at the core of the jet would lead to higher density and consequently reduced axial velocity; conversely, a richer mixture at the outer shear layer would result in decreased density and increased axial velocity, since the density of methane is considerably lower than that of air.

In conclusion, due to the intricate nature of the

phenomenon under investigation, the impact of density variations on swirling flow cannot be definitively ascertained using just a single (LES).

4.4. Reactive methane case

In this section, we examine the analysis of the reactive full methane LES. Additionally, a preliminary analysis is conducted to assess the emission of nitrogen oxide (NO). This analysis includes a comparison between the experimental results, the estimated NO values from tabulated data, and the performance of an alternative model that incorporates an additional transport equation for the NO mass fraction and provide modeling for its reaction rate, which is splitted in a source and a sink term that depends on the concentration of NO itself and requires thus modeling. The methodology used in this is extensively described in the work by Pitsch et al. [2].

4.4.1 Validation against PIV

Figure 5 presents a comparative analysis of the axial velocity's radial profile at various streamwise positions within the combustion chamber. It is evident that the LES fails to properly estimate the velocity magnitude at any location inside the combustion chamber. However, the precise location of the peaks in the radial position of the axial velocity is captured quite accurately, particularly at initial axial locations. Furthermore, accurate prediction of the minimum velocity of the CRZ is seen downstream from the first axial position. The observed discrepancy between the reactive and non-reactive cases, where the PIV profiles where predicted very accurately by the LES, may be attributed to a variety of factors.

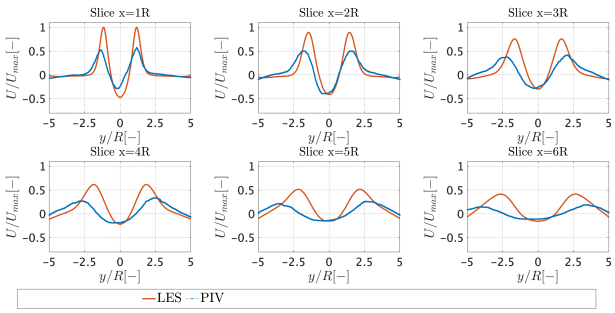

Figure 5: LES Favre-filtered time-averaged radial distribution of the axial velocity against PIV.

In the context of reactive systems, the interplay between chemistry and turbulent swirling flow is a complex phenomenon. The acceleration of the mixture across the turbulent flame brush is influenced by thermal expansion. This acceleration is dependent upon the temperature field, which in turn is affected by the distribution of mixture fraction, that is a determining factor in controlling the local heat release. On top of this, the assumption of adiabatic walls plays a significant role in this context. It should be noted that the simulated temperature field tends to be higher than the experimental results due to the neglect of heat losses to the surrounding environment and, far more importantly, a less homogeneous mixture fraction field. These heat losses are particularly significant in magnitude when dealing with the elevated temperatures associated with methane combustion, even in a lean configuration. The unaccounted heat losses may provide a partial explanation for both the higher velocities seen in the combustion chamber and the fact that experimental observation show a lifted flame, whereas the LES predicts a flame attached to the burner. Indeed, thermal losses have the effect of reducing the temperature field, hence resulting in a decrease in the turbulent flame speed. The flame is forced to stabilize in a downstream region, where a reduced flow velocity is seen as a result of the presence of the central recirculation zone. From this viewpoint, it may be deduced that the LES model is more prone to predict flashback occurrence than what happens in reality. One potential approach to improve the alignment with PIV is to implement a five-dimensional tabulation into the flamelet model. This tabulation would include the specific enthalpy, progress variable, mixture fraction, and their respective variances. This approach would enable the elimination of the assumption of adiabatic walls and include considerations for heat losses.
Nonetheless, the primary cause of the flow field misprediction is mainly attributed to the inadequate resolution of mixing: an important amount of mixing occurs in the boundary layer of the mixing tube, where it is not resolved but modeled using wall functions. This may result in a mixture fraction field that is more heterogeneous, producing zones that are richer and therefore higher in temperature. These zones have

the dual effect of increasing the mixture's acceleration and shifting the stabilization position of the flame upstream as a result of the higher turbulent flame speed. One potential method for improving mixing within the boundary layer involves modifying the employed wall functions in a manner that results in an increased turbulent viscosity ν_t. This heightened turbulent viscosity serves to enhance the diffusion of various quantities, including momentum and species mass fraction.

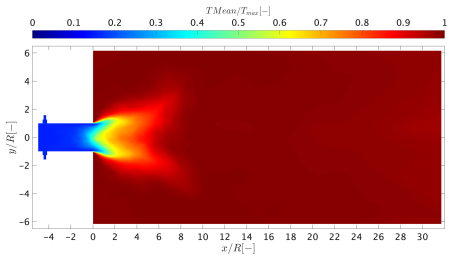

Figure 6: Mean temperature field $\langle \tilde{T} \rangle$.

4.4.2 NO_x emissions analysis

The substantial sensitivity of the source term of NO with temperature is seen in Figure 7. This sensitivity arises from the exponential dependence of the forward rate constant in the Zeldovich mechanism. The scatterplot illustrates a correlation between the proximity to the adiabatic flame temperature and the increasing significance of nitric oxide formation. This observation serves as evidence supporting that the thermal route is the primary mechanism for the creation of NO if temperatures are high enough.

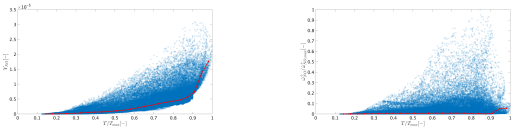

(a) (b)

Figure 7: Scatterplot of a) mass fraction of nitric oxide $\tilde{Y}_{NO}$ and b) normalized source term of nitric oxide $\overline{\dot{\omega}}^{+}_{NO}$ against adimensionalized temperature $\tilde{T}$.

Figure 8 illustrates the correlation between the source term of NO and the mixture fraction, whereby the stoichiometric value is emphasized in the color black. The range of the x-axis has been restricted to include just the flammability range of methane when mixed with air. It is evident that not only the Zeldovich mechanism is important, as we can see from the lean-fuel part, but also the prompt mechanism is playing a role in the production of nitric oxides, as the source term is elevated also in the rich region near stochiometric.

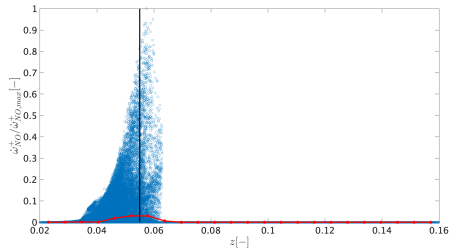

Figure 8: Scatterplot of normalized source term of nitric oxide $\overline{\dot{\omega}}^{+}_{NO}$ against mixture fraction $\tilde{z}$.

It is worth noting that achieving a fast transition between fuel-rich and fuel-lean regions is crucial for the reduction of NO_x emissions, as it helps prevent prolonged residence times near the stoichiometric condition. The attainment of this objective may be accomplished by the implementation of an efficient blending process, which is capable of achieving perfect premixing of the fuel and oxidizer prior to their introduction into the combustion chamber. The swirler serves a valuable function in this regard, as it contributes to the improvement of mixing.
Additionally, the scatterplot of the source term of NO against local flow age in conjunction with the contour plot depicting the local flow age, provides valuable insights into the specific regions inside the combustion chamber where the generation of nitric oxides occurs, as shown in report of this thesis. The production is effectively nonexistent until the fresh mixture reaches the combustion chamber, as shown by the first 20$[ms]$ of observation, which is obvious given that no reactions are occurring. Subsequently, the emission formation begins next to the burner, where the flame achieves stability, and persists at heightened levels within the central recirculation zone and outer recirculation zone. This may be attributed to the combined effects of greater temperatures and prolonged residence time. In downstream areas characterized by a local flow age exceeding 180 milliseconds, the source term of NO diminishes significantly, resulting in a cessation of production.

The predicted emissions of nitrogen oxide (NO) are about ten times lower than the expected values obtained from the retrieval from the look-up table. Specifically, when averaging throughout the outlet cross section, the former yields a value of $\langle \tilde{Y}_{NO} \rangle = 4.45e-06[-]$, while the latter yields a value of $\langle \tilde{Y}_{NOT} \rangle = 6.91e-05[-]$. The use of the transport equation technique demonstrates a significant improvement in the accuracy of the prediction, as shown by the comparison with the experimental value of $Y_{NO} = 3.7e-06$. Specifically, the percentage of error decreased from 1767.57% to 20.33%. This reduction in error leads to a value which is quite close to the actual findings, despite the fact that the flow field does not align with the experimental data in the reactive scenario. The use of pre-tabulated chemistry has dramatically limited effectiveness in accurately estimating emissions of nitric oxides. However, the research conducted in [2] significantly improves the flamelet model in addressing this issue.
The temperature sensitivity of NO, being most of it produced via the Zeldovich mechanism, suggests that the accurate modeling of the temperature by accounting for radiation and wall heat losses is of paramount importance for its prediction. Although the flamelet model used in this study does not include enthalpy as a fifth parameter and assumes adiabatic walls, the predictions obtained by large eddy simulation exhibit a good agreement with experimental findings. Figure 9 show the field of source and sink term that makes up the reaction rate of NO.

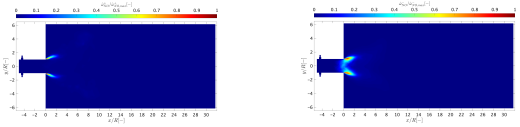

(a) Source of nitric oxides (b) Sink of nitric oxides

Figure 9: Contours of a) time-averaged normalized source term of nitric oxide $\langle \dot{\bar{\omega}}^{+}_{NO} \rangle$ and b) time-averaged normalized sink term of nitric oxide $\langle \dot{\bar{\omega}}^{+}_{NO} \rangle$.

5. Conclusions

The study aims to investigate the flow characteristics of a lean premixed combustor stabilized by a swirler, using a Large Eddy Simulation (LES) model. The LES model is calibrated for non-reactive simulations through a sensitivity analysis on the swirl number, aligning well with in-house Particle Image Velocimetry (PIV) data. Attempts to assess the impact of density variation on the flow field, specifically vortex breakdown, in a methane non-reactive case were ambiguous. The reactive LES model requires further validation for flow-field analysis, possibly related to mixing resolution. However, the model accurately predicts NO_x emissions, with a transport equation-based approach showing superiority over a tabulated method.

6. Acknowledgements

This project has been financed by the Dutch Ministry of Economic Affairs and Climate under the TKIscheme (Grant number TKI HTSM/18.0170) along with Safran SA (https://www.safran-group.com) through the APPU project (https://www.tudelft.nl/lr/appu).

References

[1] Poinsot, thierry and veynante, denis - theoretical and numerical combustion (2012).

[2] Matthias Ihme and Heinz Pitsch. Modeling of radiation and nitric oxide formation in turbulent nonpremixed flames using a flamelet/progress variable formulation. *Physics of Fluids*, 20:055110, 5 2008.

[3] Ivan Langella. Large eddy simulation of premixed combustion using flamelets, 2015.

[4] Thoralf G. Reichel, Katharina Goeckeler, and Oliver Paschereit. Investigation of lean premixed swirl-stabilized hydrogen burner with axial air injection using oh-plif imaging. *Journal of Engineering for Gas Turbines and Power*, 137, 11 2015.

[5] Thoralf G. Reichel, Steffen Terhaar, and Oliver Paschereit. Increasing flashback resistance in lean premixed swirl-stabilized hydrogen combustion by axial air injection. *Journal of Engineering for Gas Turbines and Power*, 137, 7 2015.

[6] Denis Veynante and Luc Vervisch. Turbulent combustion modeling.